RMetS

Royal Meteorological Society

The Gulf Stream and Atlantic sea-surface temperatures in AD1790–1825

G. van der Schrier* and S. L. Weber
Royal Netherlands Meteorological Institute (KNMI), De Bilt, The Netherlands

ABSTRACT: We present gridded sea-surface temperatures (SSTs) for the Atlantic basin (45 °S–60°N) as averages over the period AD1790–1825, based on early-instrumental SST data. The original measurements were compiled by Major James Rennell and made by numerous British naval vessels on behalf of the British Admiralty. We describe the digitization of this dataset and the reconstruction of spatially coherent, averaged conditions for the boreal cold (November-March) and warm (May–September) season using a reduced space optimal interpolation (RSOI) technique, in which the data is projected on a limited number of empirical orthogonal functions. This approach is validated on modern data that are sampled in a similar way as the early-instrumental data. The reconstruction for the November–March period shows a large area with anomalously high temperatures from the point where the Gulf Stream separates from the coast until *ca.* 20 °W. A tongue of anomalous cool water is found at the eastern side of the North Atlantic basin, along the coast of Europe and northern Africa. In the northeastern South Atlantic, anomalously high temperatures are found, while temperatures in the southwestern South Atlantic are anomalously cool. For the March–September season, anomalous temperatures in the South Atlantic are similar, but stronger, compared with those in the boreal cold season. Over the North Atlantic, there is not much similarity between the current SST reconstructions and those published in the late 1950s. Copyright © 2009 Royal Meteorological Society

1. Introduction

The period AD1790–1825 was the final cold episode of the so-called 'Little Ice Age', characterized by remarkable climatological conditions in the North Atlantic sector. Northwestern Europe saw very low winter temperatures and, in the westernmost areas, low summer temperatures as well (Luterbacher *et al.*, 2004).

This period was also characterized by an anomalous winter atmospheric circulation over the circum-Atlantic region in the form of a tri-pole pattern. Reconstructions of winter sea-level pressure (SLP) indicate that over Europe an anomalous low was found over the Balkan area and an anomalous high just south of Iceland (Luterbacher *et al.*, 2002). Over eastern North America, somewhat east of the Hudson bay, an anomalous low was found extending into the subtropics (Lamb and Johnson, 1959; van der Schrier and Barkmeijer, 2005). This latter low deepens the existing trough in SLP over the Newfoundland-Labrador area.

The anomalous atmospheric winter circulation led J. Bjerknes (1965) to the hypothesis that there was a change in oceanic surface flow in the northern North Atlantic, which contributed to low European winter temperatures.

In his view, frigid polar surface water was advected southward into the mid-latitudes by the anomalous surface currents. The low SSTs thus established in winter would persist into the summer season and would contribute to cool western European summers. Bjerknes' hypothesis was substantiated in a numerical study (van der Schrier and Barkmeijer, 2005) in which the winter SLP reconstruction was assimilated in a General Circulation Model. The chain-of-events hypothesized by Bjerknes was reproduced in that study.

Next to Bjerknes' hypothesis on ocean-atmosphere feedback, Lamb and Johnson (1959) and Lamb (1972) hypothesized that the position and possibly the strength of the Gulf Stream played a role in the coldness of the 1790–1825 period over Europe. According to Lamb, the North Atlantic Drift system was displaced southward and the Gulf Stream/North Atlantic Drift pursued a rather more easterly course towards the Azores in comparison with early 20th century data. Consequently, the penetration into waters north of 50°N over the eastern Atlantic was weaker, suggesting a decrease in oceanic meridional heat transport to the European mid-latitudes.

Bryson and co-workers (Bryson and Murray, 1977) also found a change in the position of the Gulf Stream during the so-called 'Little Ice Age'. By collecting early-instrumental temperature records and references from old maps of the Gulf Stream, they constructed a diagram with the direction of the Gulf Stream as it separated from

* Correspondence to: G. van der Schrier, Royal Netherlands Meteorological Institute (KNMI), De Bilt, The Netherlands.
E-mail: schrier@knmi.nl

the American continent. This diagram suggests that the heading of the Gulf Stream around AD1800 was between east and east-southeast, rather than northeast.

The evidence on which Lamb based his hypothesis is a change in Atlantic SSTs in the 1790–1825 period compared with early 20th century data. These early-instrumental SST measurements for the Atlantic (and partly the Indian Ocean) were compiled by Major James Rennell and are probably the earliest survey of water currents and ocean surface temperatures available. The survey was carried out on behalf of the British Admiralty. The data served as the basis for the celebrated Rennell current charts which map the Gulf Stream, and other ocean currents, in the Atlantic Ocean. The charts and the book (Rennell, 1832) were published posthumously by Rennell's daughter Lady Jane Rodd.

The aim of this study is to re-assess the early SST data compiled by James Rennell. More specifically, we report on the digitization of these data and present reconstructed spatial patterns of cold-season and warm-season Atlantic Ocean SST anomalies for the 1790–1825 period. We review the claim that the mean SST pattern over this period was different from the modern mean.

2. Description and digitization of the Rennell SST data

After a successful career as Surveyor-General of Bengal, appointed by the East India Company, James Rennell (1742–1830) rose to the rank of Major by 1776 and grew out to be the leading geographer in England (Pollard and Griffiths, 1993). From 1810 until his death, Rennell turned his attention to hydrography. His numerous naval friends, among which the Hydrographer of the Navy Alexander Dalrymple and Admiral Beaufort, furnished him with data in order to chart the currents of the Atlantic Ocean. Rennell extensively describes his currents charts in the covering book (Rennell, 1832). There are five charts, the first and second charts are for the eastern and western Atlantic Ocean, respectively. The third gives the 'South-African current and counter-current from the Atlantic to Indian Ocean', the fourth gives the 'connecting currents between the Atlantic and Indian Ocean' and the fifth focuses on the Gulf Stream area. On all charts, observations of SST, currents and numerous observations of wind strength and direction are plotted. Along the coasts and over banks, water depths are given and a few sightings of icebergs and data on the release and retrieval of bottles and (parts of) ship wrecks are entered. Part of the second chart, which illustrates the detail of these charts, is given in Figure 1.

Almost all of the data are from British navy vessels and collected in the period ca. 1790–1825. Attempting to gather data from other than British vessels, Rennell asked Sir Joseph Banks (then president of the Royal Society) in 1819 to approach US sources for data from ship's logs. No mention is made that American data were actually used by Rennell, suggesting that this attempt was unsuccessful (Deacon, 1980). The only American data used are taken by Dr Benjamin Franklin in 1776, 1785 and 1791 during voyages to and from the British Isles. These data are not present in the International Comprehensive Ocean-Atmosphere Data Set (ICOADS).

Rennell gives the captain's name and/or the ship's name for some of the contributions to the SST measurements in his compilation. Initially, we tried to recover the SST data directly from the ship's logs. Many of the logs could be located in the National Archives in Kew (UK), but the logs we checked did not contain the SST data we were primarily interested in. This motivated us to retrieve the SST data from the charts, which have the SST measurements entered as point values.

To digitize the SST measurements, the charts were photographed in parts with a high-resolution digital camera. The parts were then merged into one digital image for each chart. The digital version of each chart was then subdivided into small parts covering not more than ca. 10° in latitude and longitude and loaded into the UNIX program xv. In xv, the position of the SST measurements could be digitized by first determining the bitmap coordinates of each measurement, which were subsequently related to latitude–longitude coordinates. The value of the SST measurement and additional information (e.g. year, month, date, captain, etc.) were added manually. For the Rennell charts combined, this resulted in 2319 entries. Figure 2 shows the positions of these entries. The densest coverage is over the Gulf Stream region and the Agulhas region. The routes to and from the Cape of Good Hope are clearly visible. However, the data coverage over most of the Atlantic Ocean, and especially the subtropical North Atlantic, is extremely sparse.

Most of the measurements, which are labelled by both a year and a month, are organized along a known ship track, sometimes also giving information on the day or even at the time of observation. Rennell's text provides the information for some of these ship tracks. Most readings go without this information. The majority of this latter data has only the month attached to it in which the sample was taken. The mariners of those times apparently must have been aware of the seasonal cycle in SSTs, explaining the small percentage of the data (1.7%) for which it was unclear in which month they were taken. Most of the data are collected in spring and early summer (Table I). The concept of interannual variability must have been less well-known; the largest part of the data (ca. 65%) the year in which the measurement was taken is unknown. The part of the data which are labelled by a year (ca. 35%) is biased towards the 1820s (Figure 3).

The water current observations having been made from a sailing ship may be unreliable, but there is some faith in the temperature observations. Unfortunately, no details are known of how the observations were taken. It is likely that a suite of different thermometers to measure SST were used and that only after the Brussels conference in 1853 a standard practice for making
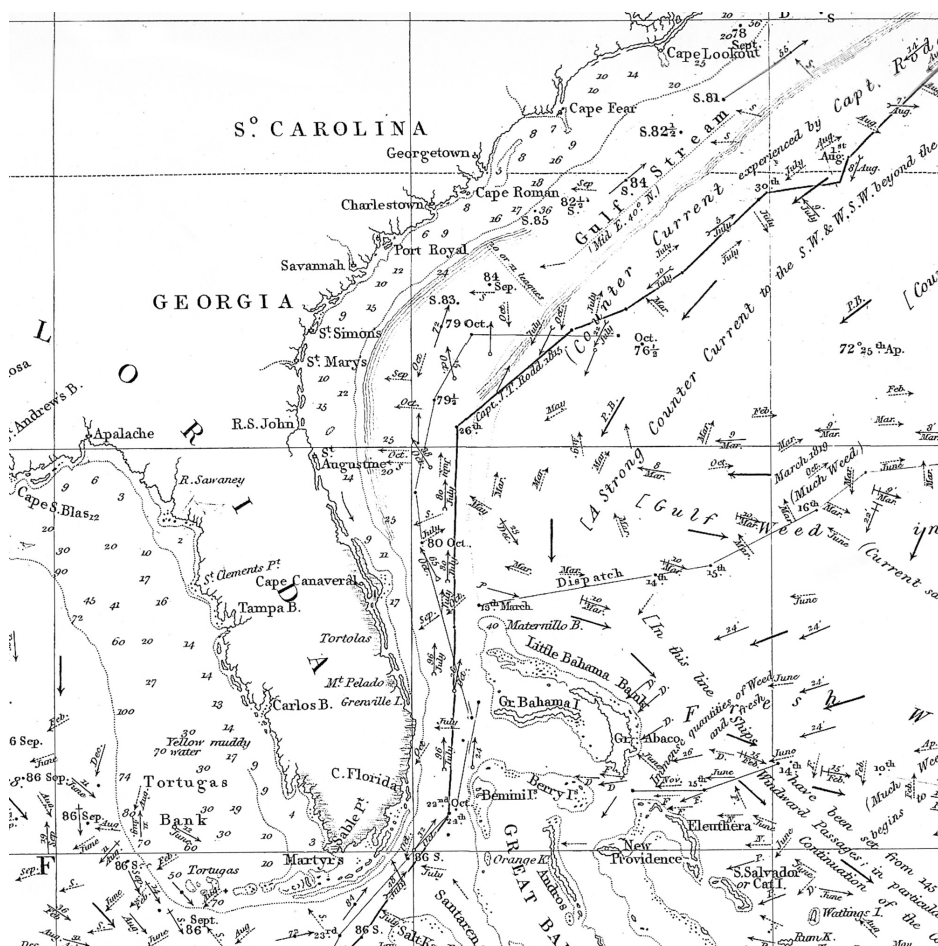
Figure 1. Part of Rennell's second chart showing the area around Florida. The bold upright numbers give the sea-surface temperature measurement (in Fahrenheit), and the month in which this measurement is taken. Some of these SST measurements are linked by a thick line denoting a ship track. Each ship track is labelled with captain and/or ship name and year. Thick arrows give current observations, thin arrows give observations of wind where the character of the arrow (dashed, solid, with feather, with open circle, etc.) label it to a ship or captain. Italic numbers give depth of the watercolumn in fathoms. Numerous and miscellaneous remarks are added to the charts.
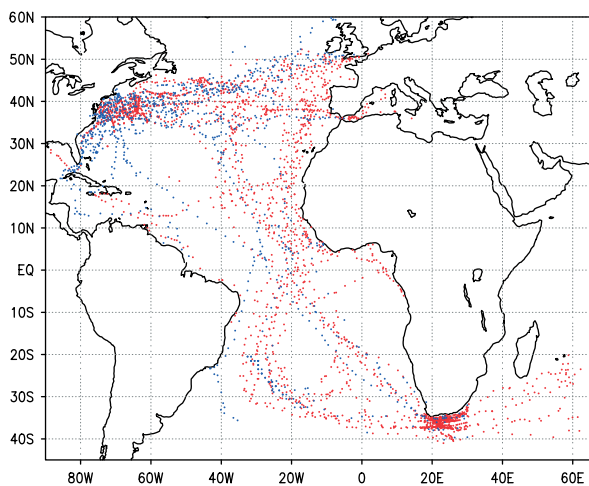

Figure 2. The locations of all entries in the Rennell dataset (red dots). The entries from the ICOADS dataset covering the 1800–1825 period, are given by blue dots.

Table I. Availability of Rennell data and early ICOADS data as a function of the month.

Month	Percentage Rennell	Percentage ICOADS
January	3.8	5.4
February	4.1	5.5
March	11.0	4.6
April	12.5	5.7
May	12.9	9.4
June	14.1	7.0
July	12.7	10.8
August	7.3	9.8
September	9.6	12.7
October	4.4	8.4
November	3.4	10.7
December	2.6	9.9
Unknown	1.7	0.0

meteorological observations was put to paper. However, these agreements were simply a continuation of the most widely used practice which suggests that the practice on board of naval vessels did not vary too much between vessels. However, an exhaustive study validating this assumption lacks. Section 4.4 compares measurements from two vessels taken nearly simultaneously and at
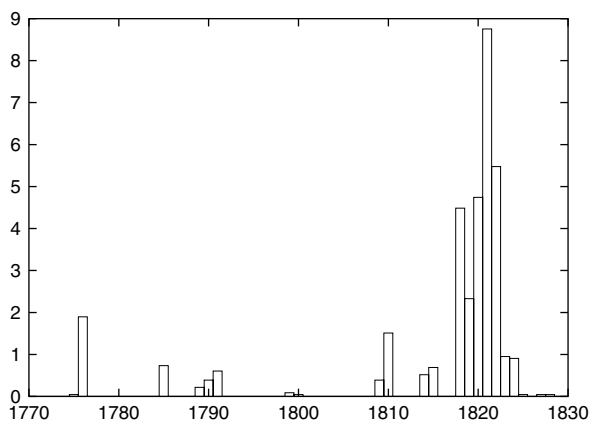
Figure 3. The percentage of data available from Rennell (1832) as a function of the year in which the measurement is taken. The subset for which information on the year in which the measurement is taken, is 35% of the total.

nearly coinciding locations.

Around the 1800s, oak buckets were in general use (Hendrik Wallbrink, personal comm.). After the 1870s, canvas buckets were widely used (Folland and Parker, 1995), replacing the wooden buckets. With sides of *ca.* 1 cm thick, the oak-buckets' walls were highly, though not perfectly, insulated. Most of the heat exchange is via the surface of the bucket. Folland and Parker (1995, their Table I (b)) give annual mean corrections for the wooden bucket between 0.08 and 0.15 °C. These adjustments are not made in the current dataset. This is motivated by the lack of supplementary data as air temperature or wind speed, making the estimate of a correction rather unreliable.

Next to the Rennell data, other data sources are available which have some data in the period of interest. These are the ICOADS data (Slutz *et al.*, 1985; Worley *et al.*, 2005) for the 1800–1825 period and the Climate World Ocean (CLIWOC) database (García-Herrera *et al.*, 2004), the latter provides a few entries only. For the period 1800–1825, the ICOADS database gives 1037 entries for the Atlantic Ocean, mostly concentrated in the year 1823.

In the following, we will analyse all the available data from the 1790–1825 period, that is the combination of the Rennell data, the ICOADS data and the CLIWOC data. In the remainder of this study, we will refer to these combined datasets as 'the early data'.

The early data is averaged in regular longitude–latitude bins of 5° × 5°. Averaging the SST readings in bins has the advantage of reducing both the observational and sampling error. Choosing 5° bins is a compromise between having a large number of entries in each gridbox while retaining enough spatial detail.

Handicapped by the absence of time control for the largest part of the data, we first average all available data on the regular grid and aim to reconstruct an AD1790–1825 *averaged* SST field for the Atlantic Ocean, subdivided in the November–March (NDJFM) and May–September (MJJAS) seasons. We do not

attempt to make a reconstruction with year-to-year variability covering the 1790–1825 period, which could then be followed by an averaging to obtain the 1790–1825 average SST field. However, it may be possible to make a reconstruction with a yearly resolution for the 1820s, since most of the data with a year and month associated are from this period. This possibility has not been pursued in this study.

The data coverage for the binned dataset with the number of entries per gridbox, for both the cold and warm season, is shown in Figure 4. This figure shows that data coverage over the entire Atlantic Ocean is better in the warm season, including the Gulf Stream region, the tropics and the South Atlantic.

3. Method

The existing approach suitable for reconstructing spatially coherent, large-scale SST patterns on the basis of sparsely sampled data is based on a combination of space-reduction methods and least-squares minimization. The large-scale features of SST are presumed to be of the largest climatic importance and are essentially all of the signal that can be robustly recovered from sparse data. Here we use the RSOI method (Kaplan *et al.*, 1997, 2000, 2003) which combines these principles and has been used earlier by Kaplan *et al.* (1997) to reconstruct Atlantic SSTs from 1856 onwards.

Other methods, like the optimal smoother or the Kalman filter or based on variational principles, cannot be applied to this problem since we do not attempt to reconstruct a time series of sequential SST fields (Kaplan *et al.*, 1997).

The simplest option, an inverse distance weighted interpolation scheme, carries information from data rich areas to areas with no data, regardless of any dynamical constraints, like cross-isothermal transport. Additionally, unrealistically high SST values in the raw data, perhaps related so some low-quality readings, are allowed to spread to infect other areas. However, the simplicity of the approach appeals and the result of an inverse distance weighted interpolation scheme is shown and discussed in the Appendix.

Here we give a brief introduction to RSOI. Let T^o be the vector of available observations of the field T with random error ε^o:

$$T^o = HT + \varepsilon^o \qquad (1)$$

Here, T is the SST field over the Atlantic, averaged over the 1790–1825 period. T^o is the SST field we have by binning all available SST readings in the gridboxes and aggregating all data to make average values for the cold and the warm season. The operator H is the matrix which puts a complete field into the format of the observations. Since T and T^o are on the same grid, H is just the 'sampling' operator: a submatrix of the identity matrix which includes only
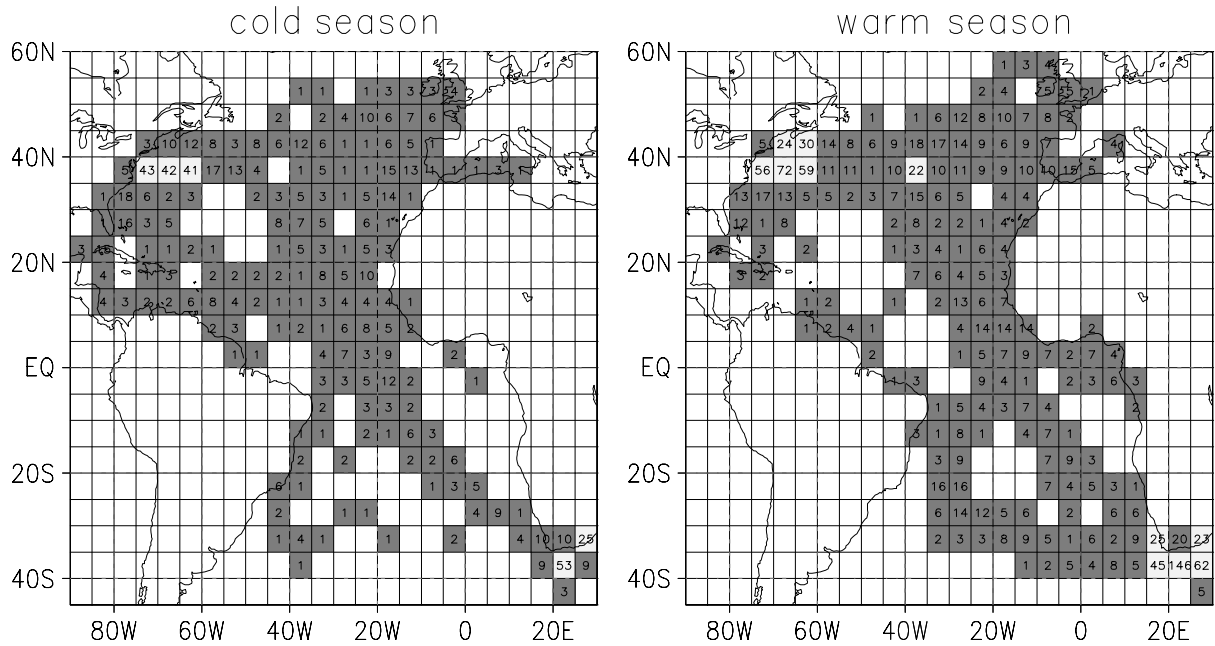
Figure 4. Coverage of the combined Rennell, early ICOADS and CLIWOC data for the cold season (left panel, November through March) and the warm season (right panel, May through September). The numbers added to the map refer to the number of entries per gridbox, gridboxes with 20 entries or less are dark grey, gridboxes with more entries are light grey. White gridboxes contain no data.

rows corresponding to the available observations. The observational error ε^o is assumed to have zero mean and known spatial covariance R. The matrix R accounts for the instrumental and sampling error in the $5° \times 5°$ box seasonal mean. It is represented by a diagonal matrix with the elements $<\sigma^2>/N_{obs}$ on the diagonal (Kaplan *et al.*, 1997). Here $<\sigma^2>$ is the intrabox measurement variability estimated through averaging over a recent, well-sampled period (1971–2000). N_{obs} is the number of observations in the box contributing to the statistics in this box, corresponding to the early period. The matrix R thus weights the gridboxes based on the number of observations in each box and the expected random error of the measurement.

We now write T as a summation over the set of spatial Empirical Orthogonal Eigenvectors (EOFs, eigenvectors of the system's spatial covariance matrix) and truncate that set to a much smaller subset which captures most of the signal. Thus:

$$T = E\alpha + \varepsilon^r \qquad (2)$$

where E is the matrix which holds the EOFs as its columns ($M \times L$ matrix, with M the number of gridpoints and L the number of retained EOFs), α is a column vector with the amplitudes of the EOFs, and ε^r designates the error due to the truncation. With Equation (2), Equation (1) can be rewritten as:

$$T^o = H\ E\alpha + H\ \varepsilon^r + \varepsilon^o \equiv \mathcal{H}\alpha + \breve{\varepsilon}^o \qquad (3)$$

The reduced space analogy of the observational error covariance matrix R is (using that ε^r and ε^o are uncorrelated)

$$\mathcal{R} = \langle (H\varepsilon^r + \varepsilon^o)(H\varepsilon^r + \varepsilon^o)^T \rangle =\rangle \langle \varepsilon^o \varepsilon^{oT} \rangle$$
$$+ H \langle \varepsilon^r \varepsilon^{rT} \rangle H^T \equiv R + HC^r H^T \qquad (4)$$

The matrix C^r is the spatial covariance matrix of SST data from the base period. In RSOI, we need to minimize the cost function (Kaplan *et al.*, 1997)

$$S(\alpha) = (\mathcal{H}\alpha - T^o)^T\ \mathcal{R}^{-1}(\mathcal{H}\alpha - T^o) + \alpha^T C^{-1}\alpha \qquad (5)$$

The first term on the right-hand-side of Equation (5) 'fits' the EOFs to the data, where the matrix $\mathcal{R}$ weights the datapoints with an estimate of the sampling error and the number of observations which contribute to each datapoint. Kaplan *et al.* (1997) provide an interpretation for the second term too. Since $\mathcal{C} = E^T C E = \Lambda$ is the diagonal matrix of eigenvalues in the reduced space, we have:

$$\alpha^T C^{-1}\alpha = \alpha^T \Lambda \alpha = \sum_{i=1}^{N} \frac{\alpha_i^2}{\lambda_i} \qquad (6)$$

which restrains the method from adding too much EOFs to the fit. The higher the mode, the smaller λ_i and the more severe the 'punishment' is for having a non-zero amplitude α_i.

The estimate α and its error $\mathcal{P}$ from this procedure are

$$\alpha = \mathcal{P}\mathcal{H}^T \mathcal{R}^{-1} T^o \qquad (7)$$
$$\mathcal{P} = (\mathcal{H}^T \mathcal{R}^{-1}\mathcal{H} + \mathcal{C}^{-1})^{-1} \qquad (8)$$

Kaplan *et al.* (1997) show in their Appendix A that this problem can be written as a generalized least

squares, for which it can be shown that the estimate (7) is the best linear unbiased estimator (BLUE) (Mardia *et al.*, 1979).

The RSOI method is commonly applied to reconstruct a sequence of spatial fields spanning a period, rather than the reconstruction of a time-averaged field as in the current study. The nonlinearity in the RSOI approach makes that a reversal of the time averaging and the application of RSOI will not yield similar results, i.e. the temporal average of reconstructed fields is not similar to the reconstruction of a temporally averaged field. However, a temporal average of the available data tends to reduce the truncation error ε^r (Equation 2) as more readings are added to a gridbox, since temporal averaging tends to damp small-scale variability. This may make the error estimate $\mathcal{P}$, Equation 8, for the reconstruction of a temporally averaged field *smaller* than that of the reconstruction of a field for a single season.

The use of space-reduction and the least-squares method implies that this method underestimates some of the spatial variance of the field which is to be reconstructed. By using anomalous fields, with respect to the 1971–2000 mean pattern, rather than the full SST fields, we obtain unbiased results even when variance is lost assuming normality in the anomalous fields.

4. Results

4.1. Validation of the RSOI technique

Here, we validate the reconstruction of coherent SST patterns using the RSOI technique by applying it to data from the 1950–1969 validation period. This data is from the ICOADS (Slutz *et al.*, 1985, Worley *et al.*, 2005). Using SST anomalies with respect to the 1971–2000 reference period, we aim to reconstruct the mean Atlantic SST field, for either the MJJAS or NDJFM seasons, over the validation period. The validation dataset is based on a *random* selection of individual ship reports from the ICOADS dataset from the 1950–1969 cold- or warm-season period. The random selection of data reflects the uncertainty in time control (relating to the year the sample was taken) for the largest part of the data. In order to have a full analogue between the early-instrumental data and the ICOADS-test data, we have to take into account that the early dataset is a synthesis of data which are not independent since they are collected along ship tracks. The procedure to construct the test data ignores this interdependency of the measurements. The result is that the deviation of the test data from the (modern) climatology does not have the spatial coherence which is evident in the early-instrumental data. To mimic the interdependency of the data, a weak spatial filter is applied to the test data. The smoothed value of each gridbox is a weighted sum of the value of the gridbox and that of the eight surrounding gridboxes. The weight of the central gridbox is 5/9, the average of the surrounding gridboxes has weight 4/9.

The spatial mask used to construct the surrogate dataset is similar to that of the combined Rennell and early ICOADS data, including the number of hits per $5° \times 5°$ gridbox. This approach leads to a dataset with the same sparse coverage as the early data. By repeating this procedure, each time with a *different* random sampling, an ensemble of surrogate datasets is obtained.

The dataset on which the most dominant EOFs of Atlantic SST are based is the gridded monthly mean data from the Hadley Centre Sea Ice and SST data set (HadISST1) (Rayner *et al.*, 2003). These data are available on a $1° \times 1°$ resolution and are regridded to a $5° \times 5°$ resolution grid. The EOFs are calculated over the 1971–2000 period based on monthly anomalies from the seasonal cycle. These EOFs will be used in the RSOI method, for both the validation and the reconstruction.

The closeness of fit is given in terms of the norm of the difference between the actual mean SST field for the control period 1950–1969 and its reconstruction:

$$\frac{1}{M}\sqrt{(E\alpha - \mathcal{T})^T(E\alpha - \mathcal{T})} \tag{9}$$

with M the number of gridboxes for which a reconstruction is produced. Here the norm is evaluated over the complete Atlantic basin, over the part north of 30°N, between 30°N and 30°S, and south of 30°S.

4.1.1. November–March season

Figure 5 shows the distribution of the norm (9) for 100 surrogate datasets, and for various truncations. In this figure, we observe that an optimal choice for the dimension of the reduced space N depends on the region one is most interested in. It also shows that the area south of 30°S is the most difficult area to get reconstructions which resemble the control SST field. Figure 5(b) suggests that $N = 25$ is the optimal choice for the northern area. Overall (Figure 5(a)), reducing the dimension to either 25, 30 or 35 EOFs gives comparable results in terms of closeness of fit. Given the scarcity of measurements in the South Atlantic, and the focus on the Gulf Stream in this study, we use $N = 25$ as the dimension of the reduced space.

Figure 6 shows two validation tests using $N = 25$ for the 1950–1969 cold-season validation period. The upper-left panel shows the deviation of the mean SST pattern for the control period from the modern 1971–2000 mean. This is the SST pattern the reconstructions should resemble. Figure 6(b) and (c) shows the reconstruction of this anomalous SST pattern based on surrogate datasets which proved to be the least and most strenuous tests, respectively. The norm (9), evaluated over the area north of 30°N, was smallest for Figure 6(b) and was largest for 6(c), indicating that the fit was best for the former and worst for the latter reconstruction. The lower-right panel shows an averaged reconstruction over all 100 surrogate datasets.

Figure 6 shows that the worst reconstruction still has some similarities with the anomalous SST pattern which
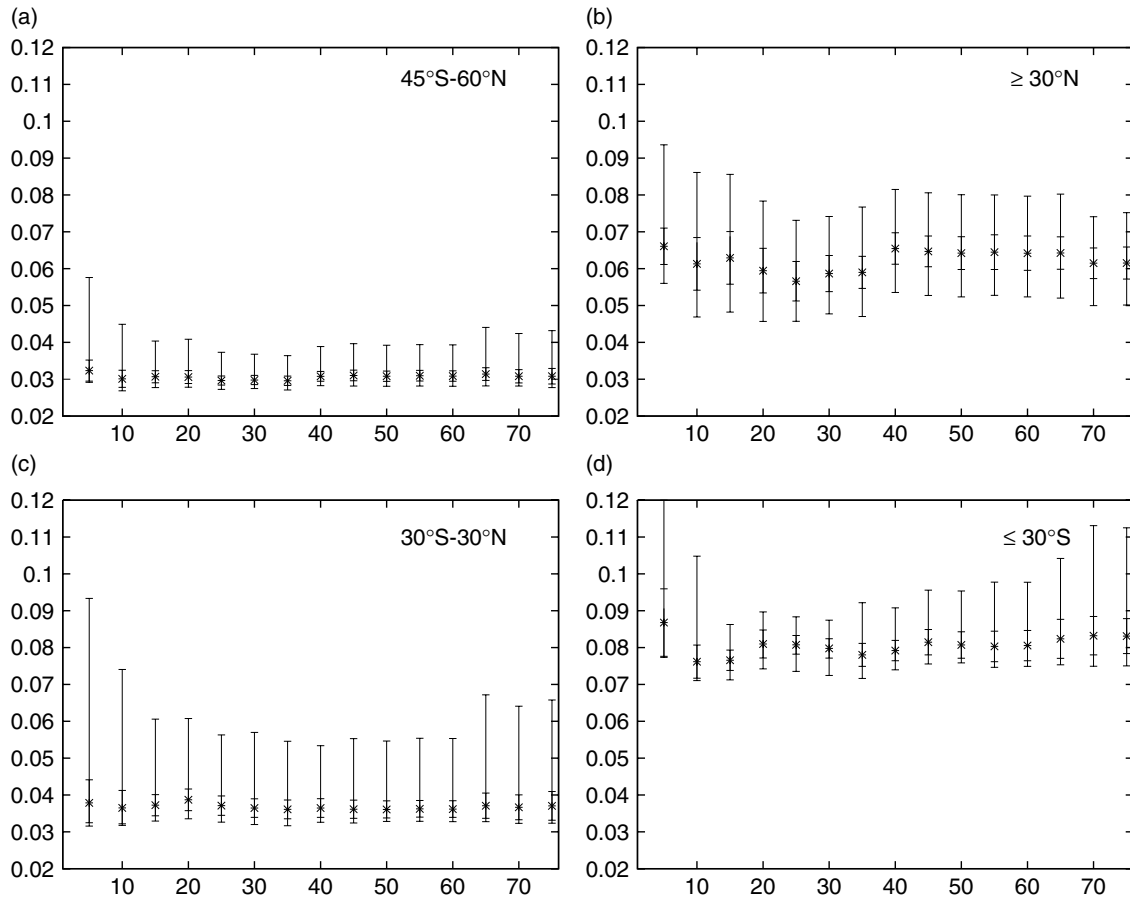
(a)

(b)

(c)

(d)

Figure 5. Box-and-whiskers plot of the distribution of the norm of the difference between the reconstruction and the 1950–1969 mean for the cold season (November–March). The asterisks denotes the median of the distribution, the maximum and minimum values of the distribution are given, as well as the median plus and minus the standard deviation. (a) Data over the complete Atlantic Ocean are used. (b) Only data north of 30°N are used; (c) shows the norm for the area between 30°N and 30°S and (d) shows the norm for the area south of 30°S.

was to be reconstructed. Higher temperatures along the eastern American seaboard are found and cooler temperatures near Europe. However, this reconstruction underestimates the warm temperatures over the Gulf Stream/North Atlantic Drift. The reconstruction which is closest to the control data has the warm area along the American coast, the cooler temperatures in the eastern part of the basin (although less extensive), and an area with cooler temperatures in the North Atlantic near 30°N. The spatial correlation between the reconstruction and the control data for the area north of 30°N is high at 0.65. Over the complete basin, the correlation reduces to 0.41.

4.1.2. May–September season

Figure 7 shows data from a similar exercise as in Section 4.1.1, but now for the May–September season. An optimal choice for the dimension of the reduced space in reconstructing the mean SST pattern in the MJJAS season turns out to be somewhat higher than that in the NDJFM season. Figure 7(b) shows a steady decrease in the median of the norm with increasing dimension, saturating at $N = 25$. Evaluated over the area south of 30 °S, saturation is reached at much higher dimension. Motivated by the same arguments as in the case of the NDJFM season, we choose $N = 30$.

Figure 8 shows the validation test using $N = 30$ for the 1950–1969 MJJAS season control period. Similar to Section 4.1.1, we show the ensemble member for which the resemblance over the area north of 30°N of the Atlantic was best (Figure 8(b)) or worst (Figure 8(c)), judged by the size of the norm evaluated over this area. Figure 8 shows that the worst reconstruction shares the warm area in the Gulf Stream region and a small cool area around *ca* 30°N with the anomalous mean 1950–1969 warm-season control period, although the amplitude of the SST anomalies is overestimated. The cool area bordering Europe's coast is replaced by warm water and not much similarity in the South Atlantic is found. The best reconstruction performs much in these respects, with cool temperatures at the eastern part of the North Atlantic and warmer temperatures, of approximately the right amplitude, over the Gulf Stream. However, the cooler conditions in the central North Atlantic of the control data, around 30°N, is deplaced slightly northward in Figure 8(b). All reconstructions show a warm pool in the eastern subtropical North Atlantic which is absent in the control data. Figure 8(d) shows that the high temperatures off the coast of Florida, in the Caribbean and along the northeastern coast of South America, are not robustly reconstructed. The pattern correlation
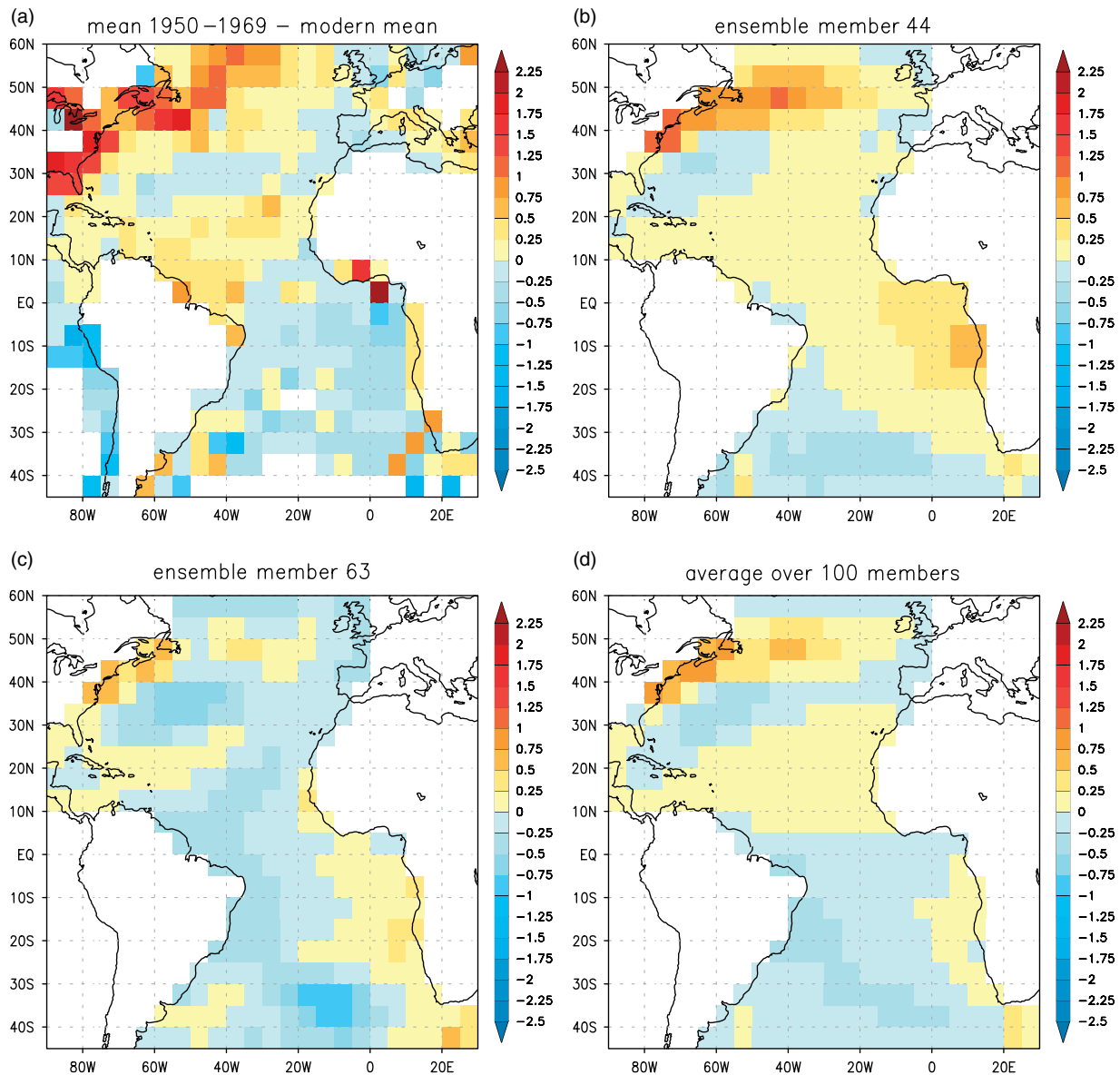
Figure 6. Validation test using $N = 25$ for the 1950–1969 control period (cold season, November–March). (a) The deviation of the mean SST pattern for the validation period with respect to the reference data. (b) The reconstruction of this anomalous SST pattern based on surrogate dataset number 44, which turns out to be the *least* strenuous test for the reconstruction method. (c) The reconstruction of the anomalous SST pattern based on surrogate dataset number 63, which turns out to be the *most* strenuous test for the reconstruction method. (d) The average reconstruction over all 100 surrogate datasets.

between the reconstruction for the SST patterns shown in Figure 8(a) and (c) is 0.51 when evaluated over the North Atlantic (north of 30°N) only.

4.2. Reconstructed early SST pattern

We now apply the RSOI technique to reconstruct the mean anomalous SST pattern for the 1790–1825 period, based on the combination of the Rennell data, the early ICOADS data and the early CLIWOC data. The same set of EOFs is used as for the calibration period, truncated at $N = 25$ for the boreal cold season and $N = 30$ for the boreal warm season. Figure 9 shows the 'raw' data (left panels) and the reconstructions (right panels), indicating that the overall structure in anomalous SST is preserved in the reconstructions. The SST amplitudes are

reduced in the reconstruction with respect to the raw data. Unrealistically, high SST amplitudes in the raw data, like in the central South Atlantic for the November–March season, are not reflected in the reconstruction.

During the NDJFM season, a large area with anomalously high temperatures is found from the point where the Gulf Stream separates from the coast up to *ca.* 20 °W. Temperatures south of the separation point are only slightly higher, up to 0.25 °C, than the modern mean. A tongue of anomalous cool water is found at the eastern side of the North Atlantic basin, along the coast of Europe and northern Africa, extending into the central subtropical North Atlantic. It will be argued below that the slightly warmer temperatures near the British Isles, contrasting with the vast area of colder waters on which
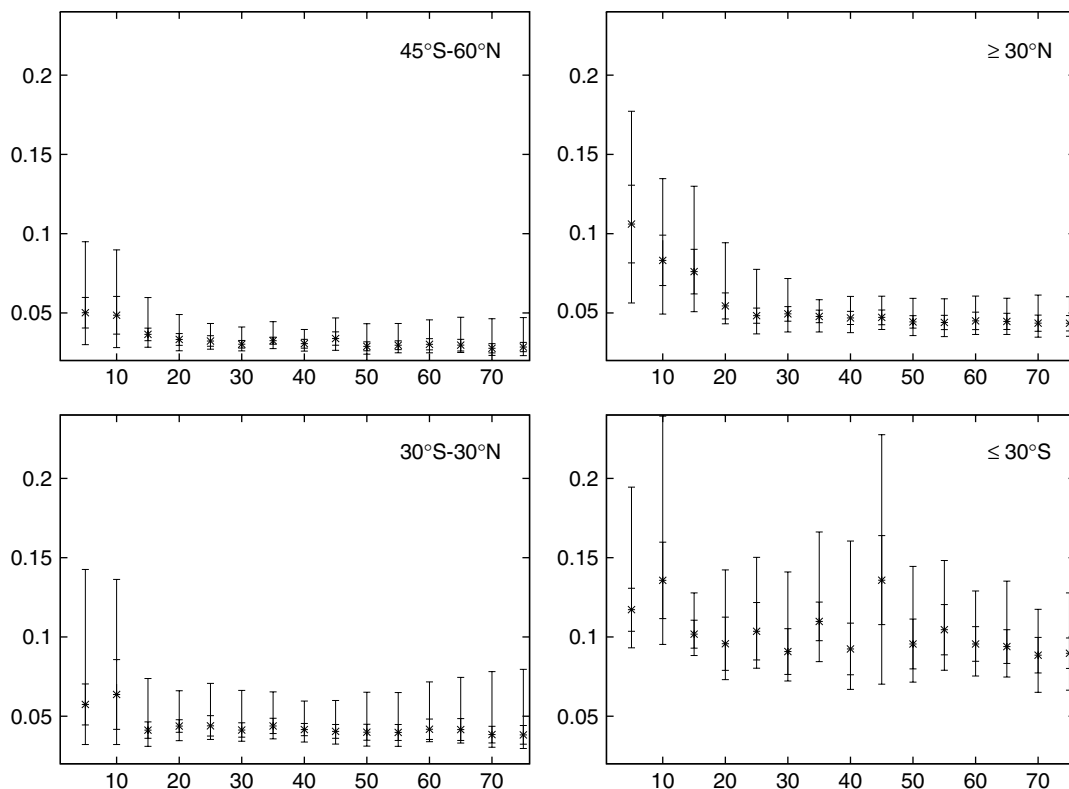
Figure 7. Similar as Figure 5, but now for the warm season (May–September).

it borders, are not robust for changes in the dimension of the reduced space.

The tropical Atlantic shows higher temperatures of up to 0.75 °C, reaching a maximum in the area of the Benguela current, with anomalous temperatures of up to 1 °C at the coast of Africa near 15 °S. This warming in the northeastern South Atlantic is mirrored in a (weak) cooling in the southwestern South Atlantic.

The anomalously high temperatures over the Gulf Stream region persist into the warm season, although the amplitude decreases. An area with high temperatures of up to 1 °C is found centred around 40°N and 25 °W. The areas with higher SSTs in the central North Atlantic and over the Gulf Stream area are connected.

In the warm season, the tropical and subtropical North Atlantic (south of 30°N) are cooler up to *ca*. 1 °C. In the South Atlantic, the warm area in the Benguela current persists and grows in amplitude in the MJJAS season. The cool anomaly in the southwestern South Atlantic is persistent too, and cools further to *ca*. −1 °C.

The robustness of anomalous SST patterns for variations in the dimension of the reduced space is estimated by making additional reconstructions with reduced space dimensions varying between 15 and 35 for the November–March season and between 20 and 40 for the May–September season, giving for each season ten reconstructions with lower reduced space dimension and ten reconstructions with higher reduced space dimension. We calculated, for each gridbox, the standard deviation of the 21 reconstructions, and divided this by the absolute value of the corresponding reconstruction shown in

Figure 9. The results are shown in Figure 10 and give a measure of the robustness of the reconstructions for variations in the dimension of the reduced space. Figure 10 shows that over most of the basin, and for both seasons, variations in the truncation has little effect, except at the edges of anomalies. This indicates that the spatial extent of the anomalies is less robust for variations in the truncation. This figure also shows the lack of robustness of the SST reconstruction of the few gridboxes near the British Isles.

4.3. Statistical significance of early SST pattern

To investigate to what extent the deviation in SST from the 1971–2000 reference period (Figure 9) is statistically significant, we use a simple one-sample t-test (Wilks, 1995). The null-hypothesis tested here is that the mean SST patterns shown in the reconstructions is not significantly different from 10-year mean SST patterns from the ICOADS database, taken over the 1990–1999 period. Although 20 or 30-year averages would be more appropriate, we use 10-year averages to increase the sample size. The statistical significance estimates will thus be somewhat too cautious.

Figure 11(a) shows the confidence levels for the November–March and May–September seasons. It shows that the change in temperatures is most significant at the eastern side of the North Atlantic basin, extending into the central subtropical North Atlantic, where the null-hypothesis can be rejected with up to 95% confidence. The warming over the Gulf Stream immediately downstream from the separation point in the boreal cold
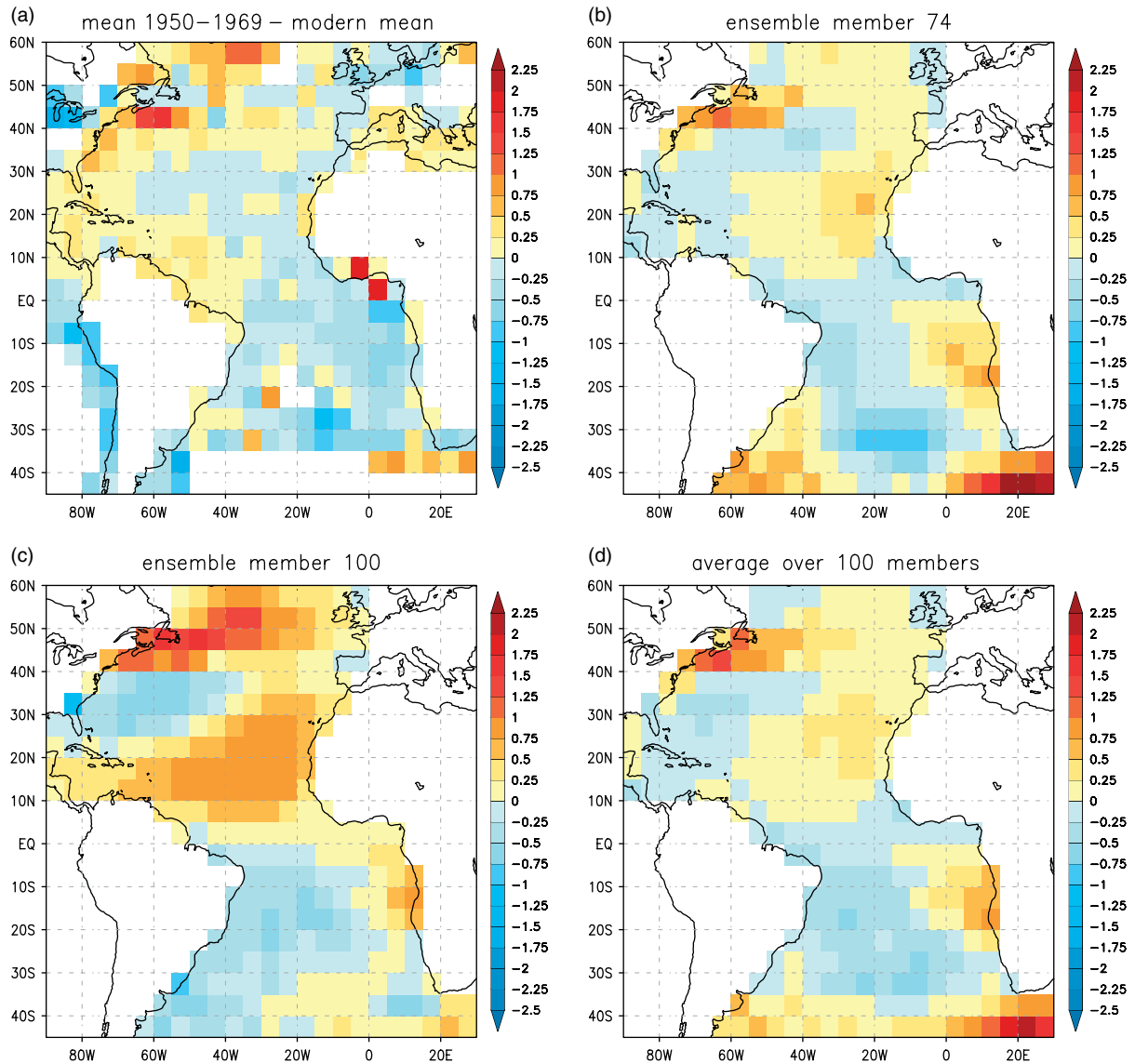
Figure 8. Similar to Figure 6, but now for the warm season (May–September). The dimension of the reduced space is $N = 30$. The lower-left (upper-right) panel shows the validation test of the ensemble member which turns out to be the most (least) strenuous test for the reconstruction method.

seasons fails to be significant, while the modest change in temperatures upstream from the separation point has some significance.

In the South Atlantic, temperatures at the southwestern tip of Africa are different from modern values with some confidence, as well as temperatures along the Atlantic seaboard of South America. The strong temperature changes in the Gulf of Guinea and around 30 °S, 20 °W fail to be statistically significant.

Figure 11(b) shows that the most statistically significant SST changes are to be found in the North Atlantic, with the exception of an area centred around *ca.* 40°N, 30°W.

4.4. Examples of measurements along tracks

Figure 12 shows a selection of the tracks in the Rennell dataset which are in the vicinity of the Gulf Stream. Table II relates these tracks to a captain and/or ship and a month and year. Some of these tracks are made with the sole purpose of charting the Gulf Stream, others are made by 'ships of opportunity' on their outset or homeward journeys.

Some of these purpose-made tracks are tracks H and I in Figure 12, made by Mr B. and Mr Napier respectively (we do not have information on the identity of Mr B.). The tracks nearly coincide and the track made by Mr B is made between 18 May and 27 May in southward direction, Mr Napier's track is made between May 17 and 18 May in northward direction in the year 1821. The near overlap of (part of) the measurements along these tracks allows a comparison of the measurements (Figure 13). This figure shows that for the northern part of the tracks, the measurements are comparable, with the difference between the readings decreasing as the distance between the tracks decrease. Further south, where the tracks diverge and the synchronicity
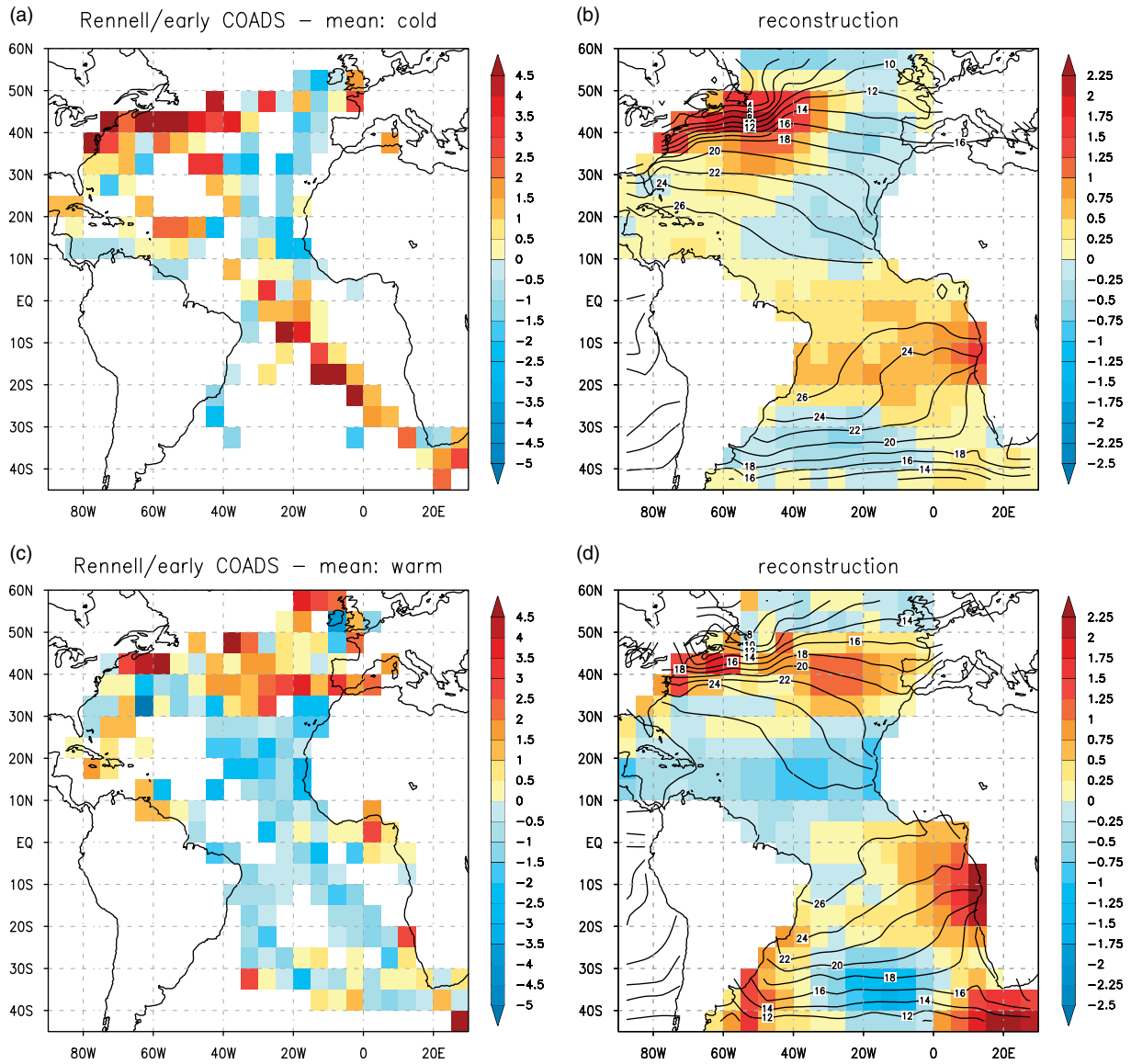
Figure 9. The mean SST anomalies for the 1790−1830 period, based on the combination of the Rennell data and the early ICOADS data; (a) The 'raw' data as a deviation from the 1971−2000 period mean for the cold season (November−March). (b) The reconstructed pattern. The dimension of the reduced space is $N = 25$. The lower panels are similar to the upper panels, but now for the warm season (May−September). The dimension of the reduced space is $N = 30$. The contours in the right panels denote the mean 1971−2000 SST pattern for the corresponding season (contour interval 2 °C).

in observation time lacks, the difference in readings increases. This comparison shows that for these tracks, measurements made at different ships are comparable, which adds to the confidence in the Rennell dataset.

To illustrate a possible northward shift of the Gulf Stream system as an explanation of the warm anomaly in the boreal cold season shown in Figure 9, we show SST measurements from tracks made in this season. These early SST measurements are compared with SST readings from the ICOADS database. ICOADS-SST data from the corresponding month from the 1971−2000 period are binned on a high-resolution 0.5° × 0.5° grid. Gridboxes are then coupled to early SST readings when the early measurement is taken in that particular gridbox. Figure 14 shows the mean value of the modern readings with error bars showing the mean plus/minus one

standard deviation. The data along the tracks are organized from south to north, or, if the track has a distinct zonal orientation, the readings are organized from west to east. The high values of the standard deviation indicate that this area has highly variable SSTs. Figure 14 shows that track D (March 1821) shows anomalously high SSTs for the southern part of the track, and anomalously low readings for the northern part. A clear shift in position of the SST gradient between the early and the modern data cannot be distinguished. The SST readings along track J (February 1820) do not show a frontal structure, and the early readings are (mostly) within the range of the modern data. The early SST data along track L (November 1776) show consistently higher SST measurements than their modern equivalent. Tracks D and L thus suggest a *warmer* Gulf Stream rather than a shift northwards.
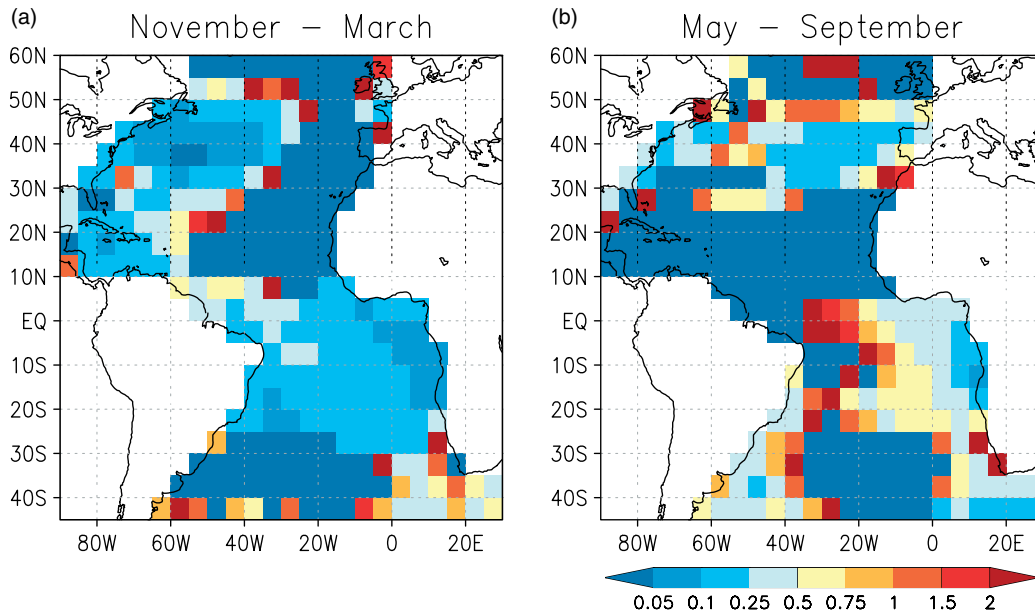
Figure 10. A measure for the robustness of the SST reconstruction of Figure 9. Shown is the standard deviation of 21 reconstructions; ten reconstructions having lower dimension of the reduced space and ten having higher dimension of the reduced space. For the November–March season, the dimension varies between $N = 15$ and $N = 35$, for the May–September season, the dimension varies between $N = 20$ and $N = 40$. The lower the standard deviation, the more robust the reconstruction of Figure 9 is for changes in the dimension of the reduced space.
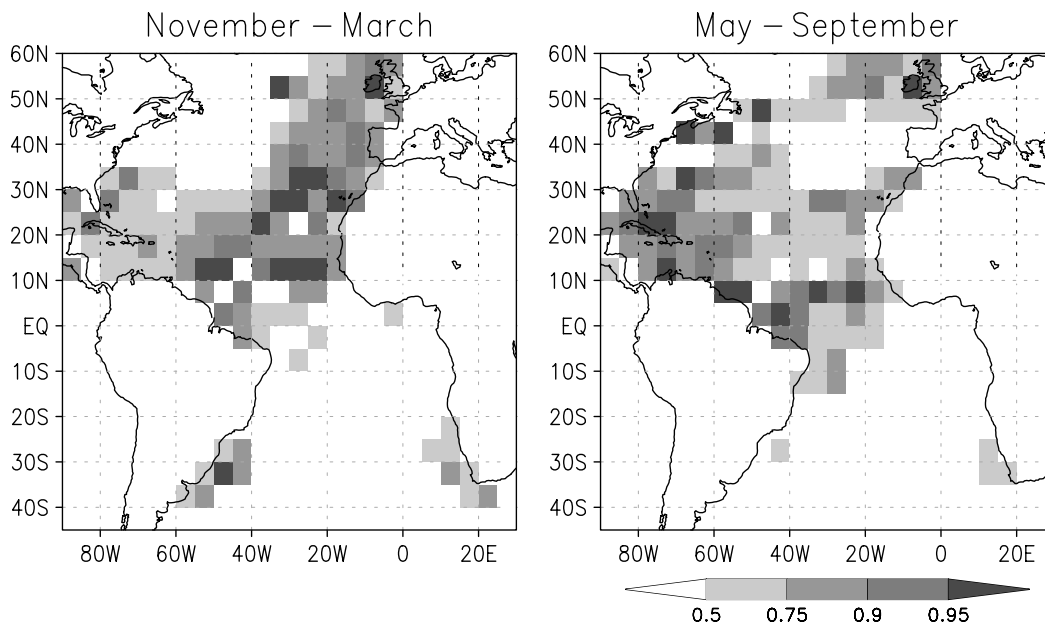

Figure 11. Confidence levels that the SST reconstructions of Figure 9 are significantly different from modern 10-year averaged mean SST patterns.

The SST readings along the remaining tracks are shown in Figure 15 and confirm the boreal warm-season SST reconstruction of Figure 9 that temperatures in the Gulf Stream area for this season are not vastly different from modern values.

5. Discussion and conclusions

The anomalously high temperatures over the Gulf Stream area in the November–March and May–September

season seem to indicate a *northward* shift of the Gulf Stream system after having separated from the coast. Even a modest northward shift would account for a rise in temperature of *ca.* 2.5 °C, given the steep cross-stream temperature gradient of the Gulf Stream. This interpretation is consistent with earlier SLP reconstructions for boreal winter (Lamb and Johnson, 1959; van der Schrier and Barkmeijer, 2005), which show an extensive anomalous low over northeastern North America, extending into the subtropical North Atlantic Ocean. Using the Sverdrup relation (Pedlosky, 1987), water under cyclonic wind

systems is forced by a positive curl of the wind stress, moving the Gulf Stream poleward.

The warm anomaly in the North Atlantic during boreal winter has some similarity with the first mode of variability in SST identified by Deser and Blackmon (1993) on the basis of COADS data from AD1900–1989. They tentatively relate the warm anomaly to a modest northward shift of the Gulf Stream.

High temperatures in the November–March season over the Gulf Stream area and a modest northward shift in the position of the Gulf Stream, tie in with Rennell's view (p.51 Rennell, 1832) that the separation point of the Gulf Stream was north of Cape Hatteras. In a letter to Admiral Beaufort (dated 4 August 1816), Rennell writes about the generally held idea of separation at Cape Hatteras: "... this is a mistake. It [the Gulf Stream] is found in 38° at the distance of 20 or more leagues, only from the shore of Maryland, setting to the NE (...) from the entrance of the Delaware. Thence it turns to ENE & EbN, NE..."

Alternatively, anomalously high temperatures over the Gulf Stream area may also indicate a stronger Gulf Stream volume transport. The few ship tracks from the
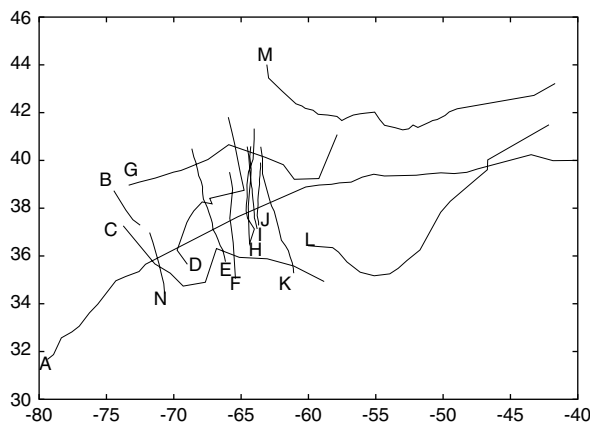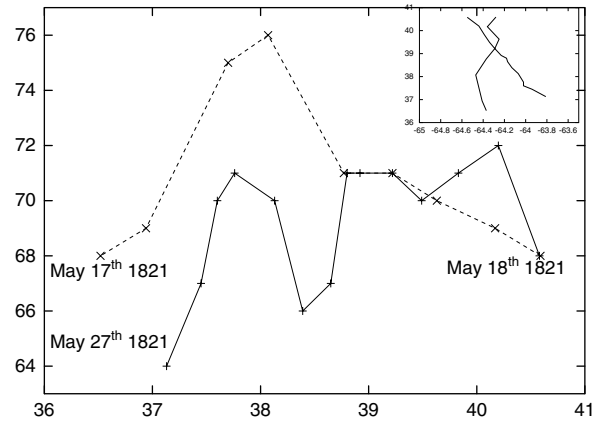

Figure 13. SST measurements (in °F) *versus* latitude for two tracks. The solid line gives a track made between 18 and 27 May 1821 by Mr B (in southward direction). The dashed line gives readings made by Mr Napier between 17 and 18 May 1821 (in northward direction). Inset shows the position of the two tracks.

Rennell dataset made in this season are suggestive of this explanation. Independent evidence suggests that the Gulf Stream volume transport may indeed have been larger in the 1790–1825 period. On the basis of early-instrumental daily temperature and daily air pressure readings (van der Schrier and Jones, 2008a, 2008b), more persistently occurring and more severe cold air outbreaks in the northeastern United States were observed in this period. The vigorous ocean-atmosphere heat exchange associated with outbreaks of frigid polar continental air over the warm waters south of the Gulf Stream, cause the formation of very deep mixed layers immediately south of the Gulf Stream (Worthington, 1972, 1977). These variations increase the pressure gradient across the Gulf Stream and account for the increase in Gulf Stream transport.

The cooler temperatures at the eastern side of the basin in the NDJFM seasons, and to a lesser extent in the MJJAS seasons too, may have been caused by enhanced advection of cool waters southward. Interestingly, cooler

Figure 12. Selection of tracks in the Gulf Stream area with SST measurements. The track labels refer to the information in Table II.

Table II. Information on a selection of ship tracks. The tracks are shown and labelled in Figure 12.

| Track	Captain	Ship	Date
A	Captain Livingstone		September 1818
B			June
C	Dr Franklin		September 1785
D	Mr B		March 1821
E	Mr Napier		September 1821
F		HMS Maidstone	18−20 June 1815
G	Dr Franklin		September 1791
H	Mr B		18−27 May &
	(two tracks made)		8−10 May 1821
I	Mr Napier		17−18 May 1821
J	Mr Napier		22−23 February 1820
K	Mr Napier	HMS Newcastle	May 1820
L	Dr Franklin		November 1776
M	Admiral Murray	Eliza Packet	May 1810
N		Sybille	April 1818
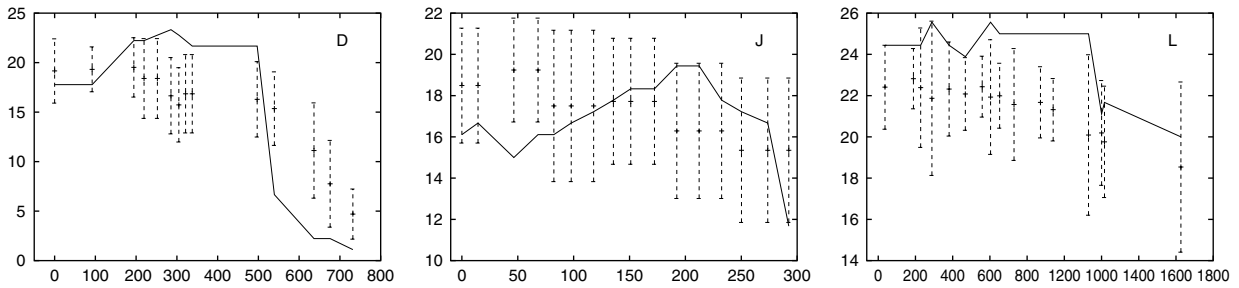
Figure 14. SST measurements along tracks D, J and L which are made in the boreal cold season (solid). The position of the tracks are shown in Figure 12. The '+' give the modern mean 1971–2000 SST equivalent with its standard deviation in the error bars. The horizontal axis denotes along track distance (in kilometres).
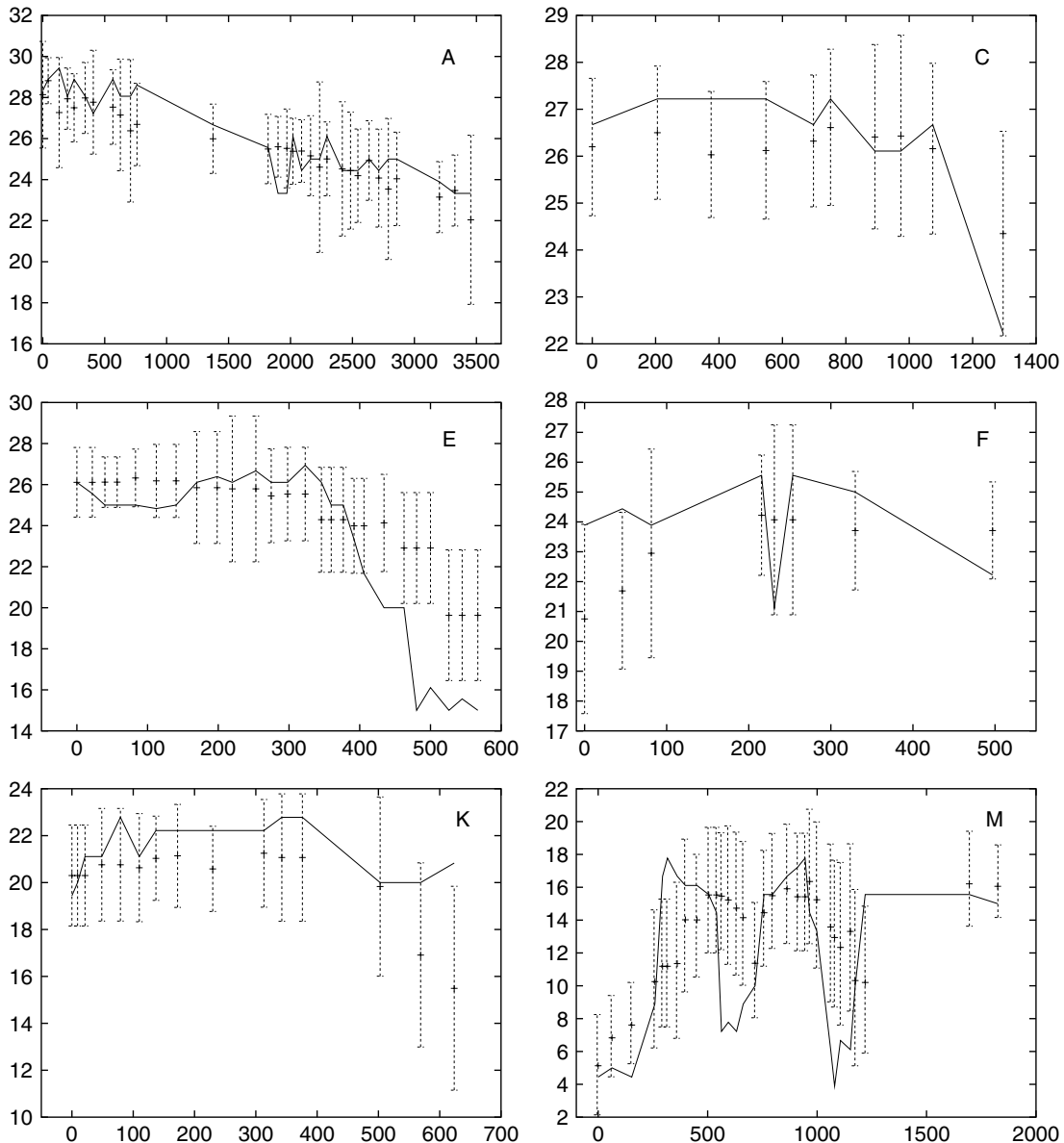

Figure 15. SST measurements along a selection of the tracks made in the boreal warm season (solid). Labels refer to tracks shown in Figure 12. The '+' give the modern mean 1971–2000 SST equivalent with its standard deviation in the error bars. The horizontal axis denotes along track distance (in kilometres).

conditions just off the west African coast at 20°N for this period are also retrieved by deMenocal *et al*. (2000) in their marine sediment records. They attribute the temperature anomaly to enhanced southward advection by the eastern boundary current or to increased regional upwelling.

The cooler NDJFM temperatures over the northeastern part of the domain are consistent with recent reconstructions of air temperature for this period (Luterbacher *et al.*, 2004; Xoplaki *et al.*, 2005). These latter reconstructions also indicate cool temperatures in the boreal warm season, which are partially reproduced here. Note that the gridboxes for which the comparison in the warm season is less favourable have also a larger uncertainty attached to them.

A proxy-based reconstruction (Mann *et al.*, 2000) of air temperatures shows a near-uniform cooling over the Atlantic basin for the 1790–1825 period for both the cold and warm season. Anomalous temperatures for most of the basin are between 0 and $-0.25\,°C$, while in the eastern South Atlantic, the cooling is slightly stronger at -0.25 to $-0.5\,°C$. A similar overall cooling pattern is found for the 1815–1825 period, which contains most of the early SST data. The Mann *et al.* reconstruction is based on terrestrial proxies only. The present SST reconstruction shows that more spatial structure is present, with warm anomalies over large areas of the Atlantic Ocean.

The pattern with anomalously high temperatures in the northeastern South Atlantic and low temperatures in the southwestern South Atlantic is consistent with a slow-down of the subtropical gyre, advecting less cold water form the mid-latitudes into the South Atlantic (sub)tropics, and advecting less warm water poleward. These latter temperature anomalies are stronger in the May–September season, suggesting an even stronger reduction in the subtropical gyre.

The reconstructed SST pattern in the South Atlantic is reminiscent of the second most dominant mode of coupled variability between SST and SLP (Sterl and Hazeleger, 2003). On the basis of this statistical relation, the reconstructed SST pattern for the March–September season shown in Figure 9 would then suggest a weakening of the South Atlantic subtropical high and an increase in SLP south of *ca.* $35\,°S$.

There is not much similarity between the SST reconstructions shown in Figure 9 and those published earlier (their Figure 13 Lamb and Johnson, 1959), especially in the North Atlantic. The northward displacement of the Gulf Stream directly downstream of Cape Hatteras is absent in the earlier reconstruction. Correspondence in the South Atlantic is better: both reconstructions show anomalous warm areas along the coast of Africa and cooler conditions in the central to southwestern South Atlantic. Nevertheless, Lamb and Johnson's (1959) and Lamb's (1972) hypothesis that the Gulf Stream/North Atlantic Drift system had a more zonal orientation seems to hold based on the current SST reconstructions for the boreal cold season. The current reconstruction does not support evidence that a similar process occurred during the boreal warm season, although a northward shift may explain the higher temperatures over the Gulf Stream downstream of the separation point.

The current SST reconstructions show a decrease in temperature for the waters bordering the European continent for the boreal cold and, to a lesser extent, warm season. This provides strong oceanographic support for the observed cool temperatures in Europe for the 1790–1825 period, as suggested earlier by Bjerknes (1965). The current reconstructions thus provide additional support for Bjerknes' view that the ocean played a significant role in shaping climate in this period.

In closing it must be readily admitted that the current reconstructions fall short on the scarcity of the original data in many areas of the Atlantic and the lack of time control. The subset of the data for which we know in which year they were collected (next to the month), suggest that the data are strongly biased towards the post-1800 period. Moreover, two major explosive volcanic eruptions occurred in this period. One with unknown source in 1809 (Robertson *et al.*, 2001) and the Tambora explosion in 1815 which preceded the well-known 'year without a summer' (Harington, 1992). The effects of these outbursts on Atlantic SST may be over-emphasized.

Digital images of the Rennell current charts, the digitized data and the reconstructions of the mean SST patterns are available from the British Oceanographic Data Centre (www.bodc.ac.uk).

Acknowledgements

Appendix

Reconstruction by simple interpolation

In the inverse distance weighted interpolation scheme, gridboxes with missing values are interpolated from surrounding non-missing values, where the weighting of the input data is inversely related to the distance between gridboxes:

$$T(\mathbf{x}) = \frac{\sum_{k=1}^{N} w_k(\mathbf{x}) T_k}{\sum_{k=1}^{N} w_k} \tag{A1}$$
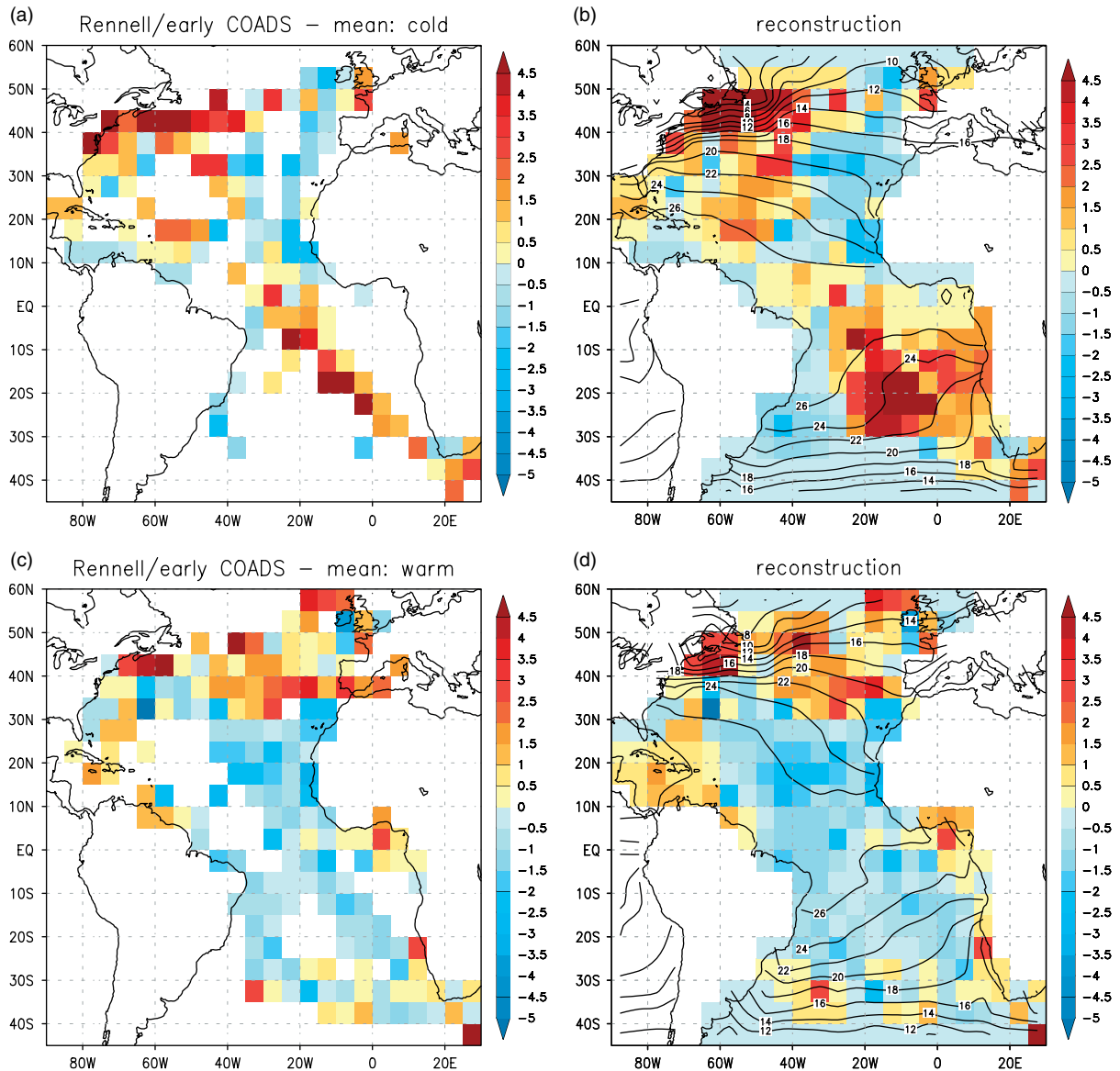
Figure A1. The mean SST anomalies for the 1790–1830 period, based on the combination of the Rennell data and the early ICOADS data. (a) The 'raw' data as a deviation from the 1971–2000 period mean for the cold season (November–March). (b) The reconstructed pattern using inverse distance weighting. The number of nearest neighbours used is 5. The lower panels are similar to the upper panels, but now for the warm season (May–September). The contours in the right panels denote the mean 1971–2000 SST pattern for the corresponding season (contour interval 2 °C).

where $T(\mathbf{x})$ is the SST value to be found at point $\mathbf{x}$, T_k are the known SST values surrounding this point and w_k is the weight. The latter is determined by:

$$w_k(\mathbf{x}) = \frac{1}{d(\mathbf{x}, \mathbf{x_k})} \qquad (A2)$$

where d is the Euclidean distance between points $\mathbf{x}$ and $\mathbf{x_k}$.

The inverse distance weighted interpolation scheme, carries information from data rich areas to areas with no data, regardless of any dynamical constraints, e.g. cross-isothermal transport. Additionally, unrealistically high SST values in the raw data, perhaps related so some low-quality readings, are allowed to spread to other areas.

For the application here, we tested several choices of N, the number of surrounding gridboxes to be used for interpolation. Larger values of N tend to smooth the reconstruction by spreading the information over greater distances, smaller values of N tend to make the reconstruction less smooth. The value of N we used here is 5.

Furthermore, in order to prevent anomalies in the upper-most northern and southern areas from spreading polewards, which would be an unrealistic feature and related to the interpolation only, we set the northern and southern most row of gridboxes of the domain to the climatological value.

Figure A1 shows the SST reconstruction based on the simple interpolation method. Overall, the reconstruction based on simple interpolation has a higher amplitude

(related to the absence of any fitting) and is spatially less smooth than the RSOI-based reconstruction of Figure 9. The first observation is related to the loss of variance associated with the fit used in RSOI, the second is related to the use of EOFs in the fit. The dominant modes of variability captured in the EOFs are spatially smooth structures. Nevertheless, the patterns are similar between the two reconstructions. In boreal winter a similarly warm Gulf Stream area and a cooler eastern North Atlantic. In the central South Atlantic, the simple interpolation-based reconstruction shows an area with anomalously high temperatures which is less evident in the RSOI-based reconstruction.

In the boreal warm season, the pattern of high anomalous SSTs over the Gulf Stream area extending towards Spain is similar between the two reconstructions. The largest differences are found in the South Atlantic, where the interpolation-based reconstruction gives overall slightly negative values, with isolated areas with positive anomalies. The RSOI-based interpolation has some pronounced positive anomalies in the South Atlantic. Note that the location of these anomalies coincide with the areas for which the robustness of the RSOI-based reconstruction is less strong (Figure 10).

References

Bjerknes J. 1965. Atmosphere-ocean interaction during the 'Little Ice Age'. In *WMO-IUGG Symposium on Research and Development Aspects of Longe-Range Forecasting*, WMO-No. 162. TP. 79, Technical Note No. 66, World Meteorological Organization: Geneva, Switzerland; 77–88.

Bryson RA, Murray TJ. 1977. *Climates of Hunger*. The University of Wisconsin Press: Wisconsin.

Deacon M. 1980. Some Aspects of Anglo-American Co-operation in Marine Science, 1660-1914. In *Oceanography: The Past*, Sears M, Merriman D (eds). Springer-Verlag: New York, 101–113.

Deser C, Blackmon ML. 1993. Surface climate variations over the North Atlantic ocean during winter: 1900–1989. *Journal of Climate* **6**: 1743–1753.

Folland CK, Parker DE. 1995. Correction of instrumental biases in historical sea surface temperature data. *Quarterly Journal of the Royal Meteorological Society* **121**: 319–367.

García-Herrera R, Wheeler D, Können GP, Koek FB, Jones PD, Prieto MR. 2004. CLIWOC final report. Technical Report UE contract EVK2-CT-2000-00090, Universidad Complutense de Madrid. Available from Dto. Fã-sica de la Tierra II, Facultad de Fã-sicas, Universidad Complutense de Madrid, Ciudad Universitaria, 28040 Madrid, Spain.

Harington CR (ed). 1992. *The Year Without a Summer? World Climate in 1816*. Canadian Museum of Nature: Ottawa.

Kaplan A, Cane MA, Kushnir Y. 2003. Reduced space approach to the optimal analysis interpolation of historical marine observations: Accomplishments, difficulties, and prospects. In *Advances in the Applications of Marine Climatology: The Dynamic Part of the WMO Guide to the Applications of Marine Climatology*, WMO/TD-1081, JCOMM Technical Report No. 13. World Meteorological Organization: Geneva, Switzerland, 192–216.

Kaplan A, Kushnir Y, Cane MA, Blumenthal MB. 1997. Reduced space optimal analysis of historical data sets: 136 years of Atlantic sea surface temperatures. *Journal of Geophysical Research* **C13**: 27835–27860.

Kaplan A, Kushnir Y, Cane MA. 2000. Reduced space optimal interpolation of historical marine sea level pressure: 1854-1992. *Journal of Climate* **13**: 2987–3002.

Lamb HH. 1972. *Climate: Present, Past and Future: Fundamentals and Climate Now*, vol. 1, Methuen: London.

Lamb HH, Johnson AI. 1959. Climatic variation and observed changes in the general circulation. Part I and Part II. *Geografiska Annaler* **41**: 94–134.

Luterbacher J, Dietrich D, Xoplaki E, Grosjean M, Wanner H. 2004. European seasonal and annual temperature variability, trends, and extremes since 1500. *Science* **303**: 1499–1503.

Luterbacher J, Xoplaki E, Dietrich D, Rickli R, Jacobeit J, Beck C, Gyalistras D, Schmutz C, Wanner H. 2002. Reconstructions of sea level pressure fields over the eastern north Atlantic and Europe back to 1500. *Climate Dynamics* **18**: 545–561.

Mann M, Gille EP, Bradley RS, Hughes MK, Overpeck JT, Keimig FT, Gross WS. 2000. Global temperature patterns in past centuries: an interactive presentation *Earth Interactions*, vol. 4. Data available at: IGBP Pages/World Data Center for Paleoclimatology, NOAA/NGDC Paleoclimatology Program, NOAA/NGDC: Boulder.

Mardia KV, Kent JT, Bibby JM. 1979. *Multivariate Analysis*. Academic Press: London.

de Menocal PB, Ortiz J, Guilderson T, Sarntheim M. 2000. Coherent high- and low-latitude climate variability during the holocene warm period. *Science* **288**: 2198–2202.

Pedlosky J. 1987. *Geophysical Fluid Dynamics*. Springer-Verlag: New York.

Pollard R, Griffiths G. 1993. James Rennell. The father of oceanography. *Ocean Challenge* **4**(1/2): 24–25.

Rayner NA, Parker DE, Horton EB, Folland CK, Alexander LV, Rowell DP, Kent EC, Kaplan A. 2003. Global analyses of sea surface temperature, sea ice, and night marine air temperature since the late nineteenth century. *Journal of Geophysical Research* **108**(D14): 4407, DOI:10.1029/2002JD002670.

Rennell J. 1832. An Investigation of the Currents of the Atlantic Ocean. Rivington for Lady Rodd. The sea temperature characteristics for each month are entered as point values on Rennell's Current Charts, which are separate from the volume. The original Charts are in possession of the UK Hydrographic Office.

Robertson A, Overpeck J, Rind D, Mosley-Thompson E, Zielinski G, Lean J, Koch D, Penner J, Tegen I, Healy R. 2001. Hypothesized climate forcing time series for the last 500 years. *Journal of Geophysical Research* **106**(D14): 14783–14803.

van der Schrier G, Barkmeijer J. 2005. Bjerknes' hypothesis on the coldness during 1790-1820 AD revisited. *Climate Dynamics* **24**: 355–371, DOI:10.1007/s00382-004-0506-x. (Erratum: Climate Dynamics DOI:10.1007/s00382-005-0053-0.).

van der Schrier G, Jones PD. 2008a. Daily temperature and pressure series for Salem, Massachusetts (1786-1829). *Climatic Change* **87**: 499–515, DOI:10.1007/s10584-007-9292-x.

van der Schrier G, Jones PD. 2008b. Storminess and cold air outbreaks in NE America during AD 1790-1820. *Geophysical Research Letters* **35**: L02713, DOI:10.1029/2007GL032259.

Slutz R, Lubker SJ, Hiscox JD, Woodruff SD, Jenne RL, Joseph DH, Steurer PM, Elms JD. 1985. Comprehensive Ocean-Atmosphere Data Set; Release 1. Technical Report NTIS PB86-105723. NOAA Environmental Research Laboratories: Climate Research Program, Boulder. Available on-line at: http://icoads.noaa.gov/Release1/coads.html.

Sterl A, Hazeleger W. 2003. Coupled variability and air-sea interaction in the South Atlantic Ocean. *Climate Dynamics* **21**: 559–571.

Wilks DS. 1995. *Statistical Methods in the Atmospheric Sciences*, Academic Press: San Diego, USA.

Worley SJ, Woodruff SD, Reynolds RW, Lubker SJ, Lott N. 2005. ICOADS Release 2.1 data and products. *International Journal of Climatology* **25**: 823–842. Available on-line at: http://www.wmo.int/pages/prog/amp/mmop/documents/J-TR-13-REV1.html.

Worthington LV. 1972. Anticyclogenesis in the oceans as a result of outbreaks of continental polar air. In *Studies in Physical Oceanography-A tribute the Georg Wüst on his 80th birthday*, Gordon AL (ed). Gordon and Breach: New York, 169–178.

Worthington LV. 1977. Intensification of the Gulf Stream after the winter 1976-77. *Nature* **270**: 415–417.

Xoplaki E, Luterbacher J, Paeth H, Dietrich DNS, Grosjean M, Wanner H. 2005. European spring and autumn temperature variability and change of extremes over the last half millennium. *Geophysical Research Letters* **32**: L15713, DOI:10.1029/2005GL023424.